PROCEEDINGS OF SCIENCE

SMOG at LHCb: experimental results

Elisabeth Maria Niel, on behalf of the LHCb collaboration[a,*]

[a] *École Polytechnique Fédérale de Lausanne, Route Cantonale, 1015 Lausanne, Switzerland.*

E-mail: elisabeth.niel@epfl.ch

We report the latest results obtained by the LHCb experiment in its fixed-target configuration using the System for Measuring Overlap with Gas (SMOG). These results use the pHe (2016), pNe (2017) and PbNe (2018) samples collected at a center of mass energy of $\sqrt{s_{\mathrm{NN}}} = 110$ GeV and $\sqrt{s_{\mathrm{NN}}} = 68.5$ GeV (for pNe and PbNe) respectively. The implications of these experimental results on theory are discussed, with a focus on the impact on quantum chromodynamics (QCD) and on theoretical predictions on the antiprotons flux originating from cosmic rays spallation on the interstellar medium.

The Tenth Annual Conference on Large Hadron Collider Physics - LHCP2022
16-20 May 2022
online

*Speaker

PoS(LHCP2022)150

1. Introduction

The LHCb experiment [1] has a unique heavy ion and fixed target physics program. Since 2015 the physics reach of LHCb has been extended thanks to the SMOG system (System for Measuring Overlap with Gas) which injects gas at a pressure of $\sim 2 \times 10^{-7}$ mbar in the interaction region, transforming LHCb in a fixed-target experiment. Fixed-target collisions are selected using the knowledge of the LHC filling scheme, keeping only bunch crossings where the bunch in beam one (going towards LHCb) is filled with protons and the other bunch in beam two is empty, so that the products of the fixed-target collisions are produced towards LHCb.

The results discussed here have used the pHe (2016), the pNe (2017) and PbNe (2018) samples. The kinematic region accessible with those sample, corresponding to high Bjorken-x, allows to investigate the nuclear parton distribution functions (nPDF) in the anti-shadowing region as well as the intrinsic charm content of the nucleon [2]. Furthermore, the SMOG pHe sample has produced important outputs used to interpret the results of astrophysics experiments [5]. Those results will be discussed in the following.

2. Charmonium production in pNe collisions at $\sqrt{s_{\mathrm{NN}}}$ = 68.5 GeV

Charmonium is a smoking gun for QGP (quark gluon plasma) production via the colour screening mechanism, which has been predicted more than 30 years ago in Ref. [6]. This mechanism predicts the suppression of the $c\bar{c}$ bound states under the effect of QGP. Even though the J/ψ suppression has been confirmed, the underlying mechanism cannot be completely understood due to cold nuclear matter effects (CNE) and statistical recombination effects at higher center of mass energies. More measurements at different energies and with different colliding systems are fundamental to shade lights on the CNE, such as nPDFs [4] or comovers [3]. An additional measurement has been recently provided by LHCb, where the charmonium production has been studied using the pNe sample at $\sqrt{s_{\mathrm{NN}}}$ =68.5 GeV. The signal yield is approximately 4542 for J/ψ and 76 for $\psi(2S)$, both reconstructed using the di-muon channel. The differential cross-section as a function of the center-of-mass rapidity y^* is shown in Figure 1 (left). The HELAC-ONIA [7] using CT14NLO and nCTEQ15 undershoot the data and good agreement is obtained with 1% Intrinsic Charm (IC) contribution and without it [8], hence no conclusions on the presence or not of IC can be drawn here. The total integrated cross-section has been measured to be $\sigma^{J/\psi}_{y^* \in [-2.29,0]} = 444.1 \pm 6.9\,(\mathrm{stat}) \pm 4.5\,(\mathrm{uncorr\ stat}) \pm 21.2\,(\mathrm{corr\ syst})\ \mathrm{nb}/\mathrm{A}$, where A is the target atomic mass number. This value has been extrapolated to the full phase space and when compared to other experimental results, see Figure 1 (right), it is found to follow the power law dependency seen in previous data. In addition, the production cross-section times branching fraction of the $\psi(2S) \to \mu^+\mu^-$ relative to $J/\psi \to \mu^+\mu^-$ has been measured to be $1.67 \pm 0.27\,(\mathrm{stat.}) \pm 0.10\,(\mathrm{syst.})$ % and found in line with other measurements for different values of target atomic mass number. This is the first measurement of the $\psi(2S)$ to J/ψ ratio with SMOG.

3. D^0 and J/ψ production in PbNe collisions at $\sqrt{s_{\mathrm{NN}}}$ = 68.5 GeV

The J/ψ and D^0 cross-sections have been measured for the first time in fixed-target nucleus-nucleus collisions at a center of mass energy of $\sqrt{s_{\mathrm{NN}}}$ = 68.5 GeV. The centrality in the sample has

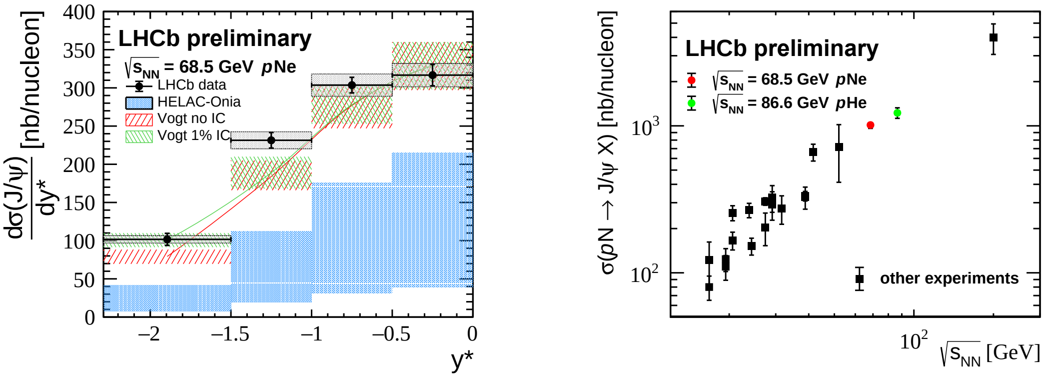

Figure 1: The J/ψ cross-section as a function of y^* (left) and the integrated J/ψ cross section compared to other experimental results from [9] (right), where the pNe result is in red. On the left figure, the predictions using the CT14NLO and nCTEQ15 PDF sets are given in blue [7], whereas the red and green boxes correspond to predictions without and with (1%) Intrinsic Charm (IC) contribution respectively [8].

been determined using the energy deposit in the electromagnetic calorimeter [10]. The J/ψ has been reconstructed using the di-muon channel with approximately 545 signal events, whereas for the D^0 the two-body $D^0 \to K^-\pi^+$ was used, with approximately 5670 signal events. The differential cross-section, shown in Figure 2 (left), points out a strong dependence as a function of p_T. The integrated ratio of charmonium to meson is measured to be $\frac{\sigma_{J/\psi}}{\sigma_{D^0}} = (5.1 \pm 0.4 \pm 0.9) \times 10^{-3}$.

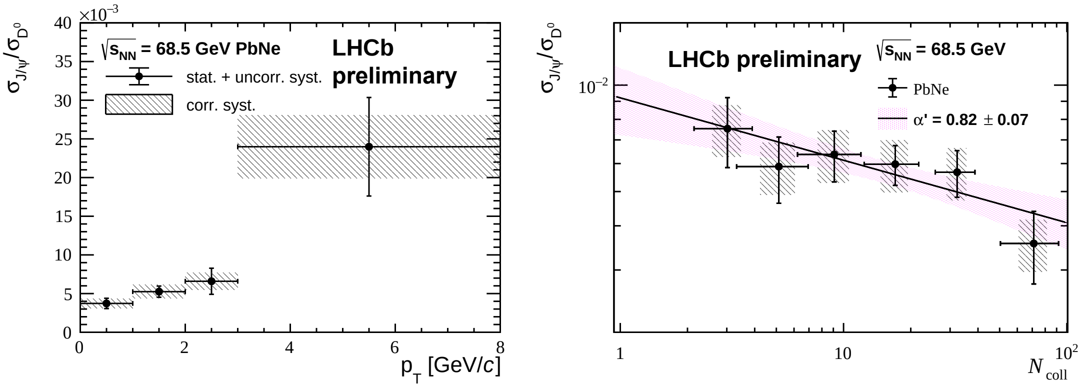

Figure 2: Ratio of the J/ψ to D^0 cross-sections as a function of p_T (left) and number of binary nucleon-nucleon collisions N_{coll} (right). The error bars represent uncertainties that are uncorrelated bin-to-bin while the boxes represent the correlated uncertainties.

The $\frac{\sigma_{J/\psi}}{\sigma_{D^0}}$ as a function of the number of binary nucleon-nucleon collisions N_{coll} (obtained from a Glauber model) has been evaluated, the results are shown in Figure 2 (right). The linear fit $\frac{\sigma_{J/\psi}}{\sigma_{D^0}} \propto N_{coll}^{\alpha'-1}$ yields $\alpha' = 0.82 \pm 0.07$ which can be interpreted as a J/ψ suppression consistent with CNE without additional QGP effects.

4. Detached antiproton production in pHe collisions at $\sqrt{s_{NN}} = 110$ GeV

The experiments PAMELA and AMD-02 have recently improved the measurements of the abundance of $\overline{p}$ in cosmic rays produced via spallation on the interstellar medium, which is composed

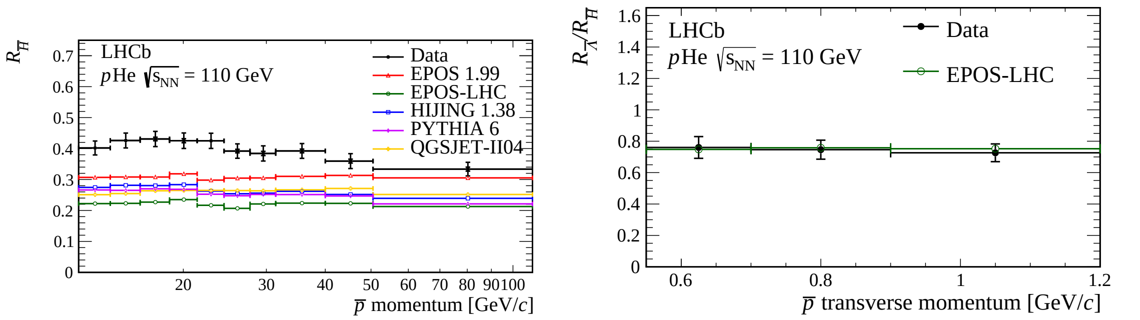

Figure 3: Measurement of the $R_{\overline{H}}$ ratio (left) and double ratio $R_{\overline{\Lambda}}/R_{\overline{H}}$ (right) as a function of the antiproton momentum. For the first, theory predictions underestimate the ratio. The second is used to prove the consistency of the analysis method by comparing to the EPOS-LHC prediction.

of mainly helium and hydrogen. This measurement requires as input the $\overline{p}$ production cross-section; indeed when comparing the data to the theoretical predictions, the uncertaitnies are dominated by the poor knowledge of the $\overline{p}$ cross-section [12]. LHCb has the unique possibility to measure the $\overline{p}$ cross-section in pHe collisions. After the first measurement of the antiproton production cross-section in the pHe sample [11], LHCb has now measured the anti-hyperon production in the same sample with the idea of measuring detached $\overline{p}$, as opposed to the prompt $\overline{p}$ of the previous measurement. The measurement is performed exploiting $\overline{\Lambda} \to \overline{p}\pi^+$ exclusive decays, where no particle identification (PID) is performed, and inclusive antihyperons decays ($\overline{\Lambda}$, $\overline{\Sigma}^-$, $\overline{\Xi}^+$, $\overline{\Xi}^0$ or $\overline{\Omega}^+$) to an antiproton and any other particle. The comparison to the prompt results is studied using the ratio $R_{\overline{H}} = \sigma(p\mathrm{He} \to \overline{H}X \to \overline{p}X)/\sigma(p\mathrm{He} \to \overline{p}_{\mathrm{prompt}}X)$. The results featuring $R_{\overline{H}}$ as a function of the $\overline{p}$ momentum are shown in Figure 3, most generators undershoot data and do not describe the momentum dependance. On the right side of the same figure the double ratio of the exlusive to inclusive measurement is shown and it is well compatible with the EPOS- LHC prediction which is known to be reliable, since it only depends on the s-quark hadronization. This proves that the method used is consistent.

5. Conclusions

The latest results obtained with the LHCb experiment in its fixed-target configuration have been discussed; those include the charmonium production in pNe collisions, the charmonium and open charm productions in PbNe collisions and the detached antiproton production in pHe collisions. For the upcoming Run 3, LHCb will operate a new gas injection system called SMOG2 [13] composed of a new storage cell allowing to locally increase the pressure of the target gas up to 35 times more than the gas pressure in SMOG. This will result in a significant increase in statistics (20 times more events with respect to the pHe sample). The LHCb fixed-target physics program will be extended even further since SMOG2 allows to inject other species of gas, including heavier noble gases, as krypton and xenon, along with non-noble species such as hydrogen, deuterium or oxygen.

The author gratefully acknowledges support by the Swiss National Science Foundation, under the grant number 185050.

References

[1] LHCb collaboration, JINST **3**, S08005 (2008).

[2] LHCb collaboration, *Phys. Rev. Lett.* **122**, 132002 (2019).

[3] E. G. Ferreiro *Phys. Rev.* B **731**, 57 (2014).

[4] K. J. Eskola, P. Paakkinen, H. Paukkunen, and C. A. Salgado, *Eur. Phys. J.* **C**, 77 (2017)

[5] LHCb collaboration, *Phys. Rev. Lett.* **121**, 222001 (2018).

[6] LHCb collaboration, *Phys. Lett.* B **178**, 4 (1986).

[7] J.P. Lansberg and H.S. Shao, *Eur. Phys. J.* **C77**, 1 (2017).

[8] R. Vogt, *Phys. Rev.* C **103**, 035204 (2021).

[9] F. Maltoni et al. *Phys. Rev.* B **638**, 202 (2006).

[10] LHCb collaboration, JINST **178**, 17 (200).

[11] LHCb Collaboration, *Phys. Rev. Lett.* **121**, 222001 (2018).

[12] M. Boudaud, Y. Génolini et al., *Phys. Rev. Research 2*, 023022.

[13] LHCb collaboration, CERN-LHCC-2019-005, (2019).